7 Continuum Angular Distributions

Coordinator: M.B. Chadwick

Summary

This chapter discusses methods for determining continuum angular distributions for use in nuclear reaction calculations and evaluated data files. We recommend the Kalbach systematics for most applications due to their wide-ranging applicability, and due to the fact that emission spectra can then be represented in a convenient compact form in evaluated data libraries. A computer code **kalbach_systematics.for** is included in the RIPL library to compute the Kalbach systematics angular distributions. We also recommend the use of a physics-based formula by Chadwick and Obložinský for analyses in which a fundamental physical derivation is preferred. A code **losalamos_analytical.for** is provided to calculate distributions with this theory. We also briefly discuss photonuclear angular distributions, and discuss how these can also be calculated using the **kalbach_systematics.for** code.

7.1 Introduction

Evaluated nuclear data files usually require a description of the angular distributions of emitted particles. The Kalbach systematics [7.1] provide a very successful characterization of these distributions, and have been widely used in evaluations. A drawback of these systematics is that they were not originally developed to include photon-induced reactions. However, Chadwick *et al.* have adapted the Kalbach systematics for use in photonuclear reactions in the quasideuteron regime (above about 40 MeV) [7.2].

A computer code obtained from Kalbach has been modified so that angular distributions in photon-induced, as well as nucleon-induced, reactions can be computed. This code, **kalbach_systematics.for**, is provided as part of RIPL.

In recent years a physics-based theory for calculating preequilibrium angular distributions has been developed by Chadwick and Obložinský [7.3]. This theory has been successfully applied in exciton model calculations [7.3], and in a Monte Carlo version of the hybrid model [7.4], and is described in some detail in the next subsection.

7.2 Theory for Preequilibrium Angular Distributions

The angular distribution of emitted particles is a subject which has attracted a great deal of interest from a physics perspective, since the angular effects give information about the underlying reaction mechanisms involved in the evolution of a quantum system towards equilibrium. Here we review some recent developments in the modeling of angular distributions which are of use in nuclear data evaluation work.

Particles ejected during the early stages of a nuclear reaction are typically of high energy and have forward-peaked angular distributions, since they are emitted prior to nuclear equilibration and partially preserve the incident projectile's direction of motion [7.5–7.11] These preequilibrium particles account for the continuum region of double differential emission spectra. Theoretical attempts to understand such spectra span from semiclassical approaches, notably exciton and hybrid models, up to recent quantum mechanical multistep theories [7.12]. The quantum mechanical approaches have been used with a certain amount of success for analyzing nucleon reactions up to 200 MeV. However, they still face open questions regarding the formulation of multistep processes [7.13], multiple particle emission, and the emission of complex particles. Semiclassical models have provided a clear insight into the physics of preequilibrium processes and have successfully explained many angle-integrated spectra, though they were initially not formulated to account for angular effects. Therefore a widely-adopted approach [7.5–7.8] is to use these angle-integrated spectra, and obtain angular distributions from the Kikuchi-Kawai [7.14] nucleon-nucleon scattering kernel in a Fermi-gas. While this has been able to explain certain features of the forward-peaking, it has not been able to account for many of the systematic properties of continuum angular distributions [7.1]. Furthermore, most works assume a fast leading-particle that carries all the directional information during the cascade. This is in contradiction to the equiprobability assumption used in the exciton model which puts all the excited particles and holes on an equal footing, and does not follow the individual particle's motion [7.6].

In the absence of a sufficient theoretical understanding of the general properties of continuum angular distributions, Kalbach developed phenomenological systematics to describe them [7.1]. She analyzed a large body of experimental measurements (over 900 data sets) in nucleon and alpha-induced reactions at energies up to several hundreds of MeV, and found simple angular variations and a surprising similarity between angular distributions in reactions involving varying types of projectile and ejectile. While these systematics are very useful for describing and predicting differential cross sections, their physical basis has remained obscure. The fact that observed continuum preequilibrium cross sections tend to vary smoothly with angle and energy, and lend themselves to simple parameterization [7.1], suggests that they should be describable using a relatively simple model of the reaction process. Here we show how momentum considerations are fundamental to the description of continuum angular distributions, and using a semiclassical preequilibrium model we derive Kalbach's parameterization of the forward-peaking shape.

An important step in reconciling the role of linear momentum in the preequilibrium cascade with the statistical assumptions of the exciton model was made by Mädler and Reif in 1980 [7.9]. They abandoned the leading particle assumption and treated the cascade in a fully statistical manner. As in the usual exciton model, it was assumed that exciton states compatible with energy conservation can be excited in a transition (so one implicitly assumes that there is mixing between particle-hole states within a given exciton class). But in addition, accessible states were restricted to those that satisfy momentum conservation. To do this the concept of the linear-momentum dependence of state densities was introduced. Recent work on exciton model angular distributions also uses this picture of the preequilibrium cascade [7.10, 7.11, 7.3]. However, the partition function technique used by Mädler and Reif to derive the state densities is impractical for numerical computations. In contrast, the approach of Refs. [7.3, 7.4] uses new and computationally tractable methods for determining the state densities with linear momentum.

7.2.1 General Features of Preequilibrium Angular Distributions

Kalbach's work [7.1] on the systematical properties of angular distributions highlighted a number of features of the measured angular distribution data that must be modeled correctly in applications:

1. The shape of a preequilibrium angular distribution has the general form of $\exp(a \cos \theta)$, where a is a parameter that governs the magnitude of the forward-peaking. Thus, when

data is plotted on a logarithmic scale against angle, it exhibits a cosine shape. This functional form for the angular distributions applies (approximately) to all types of reactions, independent of the projectile/ejectile type.

2. The a parameter is independent of target mass.

3. The a parameter is approximately independent of projectile/ejectile mass.

4. The a parameter, to a good approximation for energies up to 130 MeV, is a function of emission energy, but not incident energy.

7.2.2 State Densities with Linear Momentum

The state density with linear momentum can be expressed [7.11] as the product of a state density in energy space, $\rho(p,h,E)$, and a linear momentum distribution function $M(p,h,E,\mathbf{K})$,

$$\rho(p,h,E,\mathbf{K}) = \rho(p,h,E)\ M(p,h,E,\mathbf{K}), \tag{7.1}$$

in analogy to the usual partitioning of the angular-momentum state density. It has units of $\mathrm{MeV}^{-1}(\mathrm{MeV/c})^{-3}$, is independent of the direction of $\mathbf{K}$, and yields the energy-dependent state density when integrated over all momenta, $\int \rho(p,h,E,\mathbf{K})4\pi K^2 dK = \rho(p,h,E)$. The individual momenta of the particles and holes are oriented in random directions, and the state density with linear momentum counts all configurations which sum to the required total energy and total momentum. The Central Limit Theorem implies that the ensemble of the various particle and hole momenta sum to yield a distribution of total momenta which follows a Gaussian,

$$M(p,h,E,\mathbf{K}) = \frac{1}{(2\pi)^{3/2}\sigma^3} \exp(-K^2/2\sigma^2), \tag{7.2}$$

where σ is the momentum cut-off (representing the width of the distribution). The momentum cut-off can be obtained by considering the average-squared value of the exciton momentum projections on the direction of $\mathbf{K}$ in a Fermi-gas nucleus, giving

$$\sigma^2 = n\left(\frac{2m\epsilon_{\mathrm{av}}}{3}\right), \tag{7.3}$$

where m is the nucleon mass, $n = p + h$, and ϵ_{av} is the average exciton energy relative to the bottom of the nuclear well. Thus, as n increases with more excited particles and holes, the width of the total momentum distribution increases. If the excitation energy is less than the Fermi energy (ϵ_F) and $p \approx h$, then $\epsilon_{\mathrm{av}} \approx \epsilon_F$, but in general in an equidistant single-particle model it is given by

$$\epsilon_{\mathrm{av}} = \frac{2p(p+1)}{ng}\frac{\rho(p+1,h,\tilde{E})}{\rho(p,h,\tilde{E})} - \frac{\tilde{E}}{n} + \epsilon_F, \tag{7.4}$$

with the notation that $\tilde{E}$ denotes the excitation energy relative to the Fermi-level, $\tilde{E} = E - (p-h)\epsilon_F$, and the state densities in Eq. (7.4) are taken from the equidistant model with finite well-depth restrictions [7.15].

Recently, analogous values for the average exciton energy in a Fermi-gas (with single-particle energies increasing as the square root of energy) have been presented [7.4].

7.2.3 Preequilibrium Angular Distribution Formula

In the exciton model the emission rate from the r^{th} preequilibrium stage containing p particles and h holes, leaving p_r particles and h_r holes in the residual nucleus, is obtained by applying detailed balance. By explicitly conserving linear momentum we obtain an angle-dependent rate for emission with energy ϵ and direction Ω given by

$$\frac{d^2\lambda_n(\epsilon,\Omega)}{d\epsilon d\Omega} = \frac{2\mu\epsilon\sigma_{\text{inv}}}{\pi^2\hbar^3}\frac{\rho(p_r,h_r,E-\epsilon_\Omega,\mathbf{K}-\mathbf{k}_\Omega)}{4\pi\ \rho(p,h,E,\mathbf{K})}, \tag{7.5}$$

where for clarity we have omitted model-dependent factors which may be applied to account for the type of ejectile particle [7.12]. Here, μ is the ejectile reduced mass, and the reaction cross section for the inverse process is σ_{inv}. The composite system total energy and momentum before particle emission are E and $\mathbf{K}$, respectively, and the residual nucleus energy and momentum after emission are $E-\epsilon_\Omega$ and $\mathbf{K}-\mathbf{k}_\Omega$, respectively, all these quantities being measured relative to the bottom of the nuclear well. The energy and momentum of the emitted particle relative to the bottom of the nuclear well are $\epsilon_\Omega = \epsilon + B_{\text{em}} + \epsilon_F$ and $\mathbf{k}_\Omega$, where $|\mathbf{k}_\Omega| = \sqrt{2\mu\epsilon_\Omega}$, B_{em} being the emission particle separation energy. Momentum, like energy, is not transferred to the whole residual nucleus; rather, it is carried solely by the excited particles and holes. The forward-peaked angular variation for a given emission energy follows directly from the variation of $\rho(p_r,h_r,E-\epsilon_\Omega,\mathbf{K}-\mathbf{k}_\Omega)$ with angle Ω in Eq. (7.5). This in turn follows from the inclusion of Fermi-motion and Pauli-blocking in the state-densities, and ignores deviations from center-of-mass isotropy in nucleon-nucleon scattering. During the preequilibrium cascade the model assumes that particle-hole states can be populated providing that both energy and momentum are conserved, and the memory of the initial projectile direction is not maintained solely by a fast leading-particle, but rather it is carried by both the excited particles and the holes.

Following the preequilibrium emission of a particle with momentum $\mathbf{k}_\Omega$, the squared absolute value of the residual nucleus momentum is

$$|\mathbf{K}-\mathbf{k}_\Omega|^2 = K^2 + k_\Omega^2 - 2Kk_\Omega\cos\theta,$$

where θ is the angle of emission in relation to the projectile direction. This residual-nucleus momentum appears in the state density in the numerator of Eq. (7.5) and accounts for the angular-dependence of the emission rate. Since the cross section for emission is proportional to the emission rate, we obtain:

$$\frac{d^2\sigma_n(\epsilon,\Omega)}{d\epsilon d\Omega} = \frac{d\sigma_n(\epsilon)}{d\epsilon}\ \frac{1}{4\pi}\frac{2a_n}{e^{a_n}-e^{-a_n}}\exp(a_n\cos\theta), \tag{7.6}$$

where $d\sigma_n(\epsilon)/d\epsilon$ is the n^{th}-stage angle-integrated exciton model cross section, the pre-exponential factor arises from the normalization conditions, and

$$a_n = \frac{3Kk_\Omega}{2n_r m\epsilon_{\text{av}}}, \tag{7.7}$$

where $n_r = p_r + h_r$. The total preequilibrium emission is a sum of the above contributions for all preequilibrium stages. Conservation of linear momentum, and hence angle-energy correlation, is maintained for all orders of scattering. As would be expected, the forward-peaking increases with incident and emission energy, and decrease with increasing n as the incident momentum is shared among more particles and holes. Eq. (7.6) has exactly the same functional form that Kalbach used to describe the preequilibrium angular distributions. While the Kalbach-systematics formula is of the same functional form as the theoretical result, her expression applies to the full preequilibrium spectrum whereas the theory applies to each preequilibrium stage component. The variable "a" that she parameterized by comparisons with many measurements can be understood as an averaged value of a_n over all preequilibrium stages.

The model also provides a framework for understanding previously-unexplained features of the systematic behavior of angular distributions:

1. The angular variation as an exponential in $\cos\theta$ results from the Gaussian accessible phase space, and the vector addition of momenta using the cosine formula. The model therefore explains the general shape of measured continuum angular distributions [7.1] and its applicability to various projectile and ejectile types.
2. The independence of the angular distribution on target mass mass, since the momentum cut-off (unlike the spin cut-off) is independent of A.
3. The independence of a on projectile and ejectile mass is harder to show exactly, though possible explanations can be easily seen. In the case of composite projectiles, the increased number of excitons in the initial state due to cluster fragmentation approximately cancels the extra incident momentum. As for ejected clusters, models such as the pickup cluster model of Iwamoto and Harada include extra nucleons participating in the pick-up mechanism which again increases n.
4. The (approximate) independence of Kalbach's a parameter on incident energy below 130 MeV arises because of the approximate canceling of the incident energy dependence in the expression for a_n with the increasing number of preequilibrium stages (each with successively flatter angular distributions) that contribute.

There are similarities between this model and exciton models which use the Kikuchi-Kawai angular kernel (see Fig. 7.1). If instead of using the Gaussian (statistical) solution, the state densities with linear momentum are determined in a Fermi-gas by convoluting single-particle densities while conserving energy and momentum, the Kikuchi-Kawai result follows for 1-step scattering [7.11]. But the result for multistep scattering differs from a convolution of Kikuchi-Kawai kernels since we do not make a leading-particle assumption. We showed in Ref. [7.11] that the Gaussian solution approximates the exact Fermi-gas result very well even when the number of excitons is small. We are further encouraged to use the Gaussian solution since Reffo and Herman [7.16] found that a Gaussian angular momentum distribution described shell-model with BCS pairing calculations well, even when there are just two excitons.

7.2.4 Comparison with Measurements

Comparisons between angular distributions predicted by the linear-momentum conserving exciton model and experimental measurements have been presented in Refs. [7.3, 7.4]. Even though the model includes the quantum phenomena of Fermi-motion and Pauli-blocking, it does not account for other quantum effects such as refraction and diffraction from the nuclear potential, and finite-size effects. At low incident energies these have been shown to be important for obtaining sufficient backward-angle emission [7.6–7.8, 7.17], and result in a flatter angular distribution. A simple applications-oriented way to account for these effects is to modify a_n in Eq. (7.7) so that it is decreased by an energy-dependent parameter ζ. Writing a_n in terms of channel energies we then obtain for nucleon reactions:

$$a_n = \frac{3\,\sqrt{(\epsilon_{\text{in}} + B_{\text{in}} + \epsilon_F)(\epsilon + B_{\text{em}} + \epsilon_F)}}{\zeta\ (n-1)\epsilon_{\text{av}}}, \tag{7.8}$$

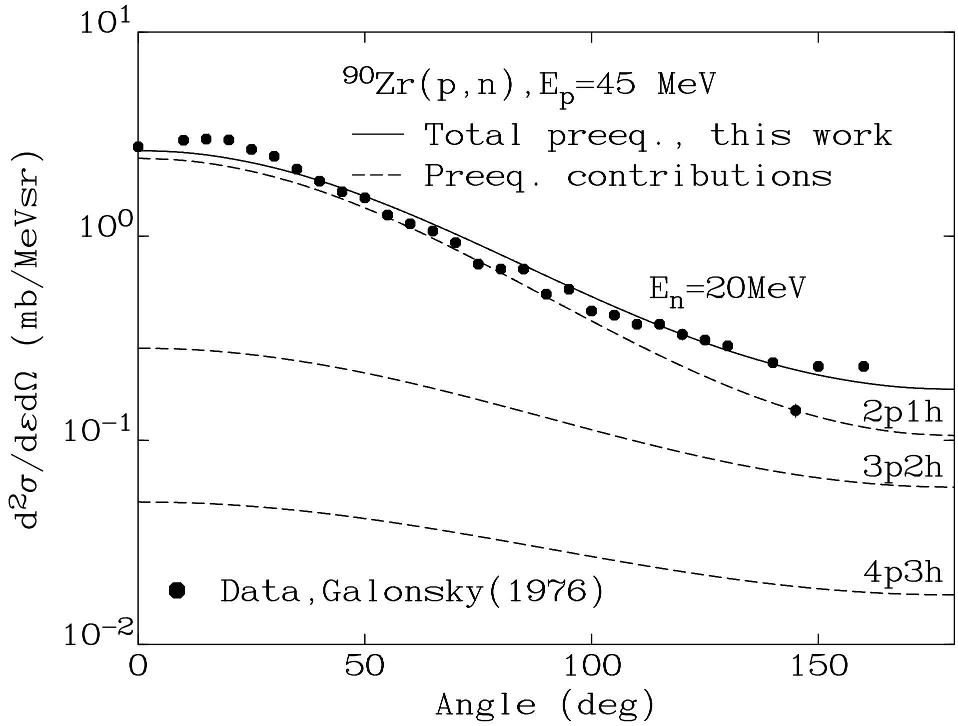

Figure 7.1: Comparison of measured (p,xn) continuum angular distributions with the theory of Ref. [7.3] applied within an exciton-model context. Data from Galonsky *et al.* [7.19]. Taken from Ref. [7.3].

and we take the Fermi-energy as 35 MeV. By analyzing a few experimental data sets we have found that the simple parameterization $\zeta = \max(1, 9.3/\sqrt{\epsilon})$, with ϵ in MeV, works fairly well up to 80 MeV. This factor tends to 1 for the higher emission energies where the quantum effects become small, and increases to 2 at 20 MeV.

Figures 7.1 and 7.2 show comparisons between prediction of the Chadwick-Obložinský theory with measured angular-distribution theory, taken from Refs. [7.3, 7.4]. The results shown in Figure 7.1 are also those used in the sample input file for the **losalamos_analytical.for** code included in the RIPL library.

7.2.5 Photonuclear Reactions

The photonuclear reaction model in Refs. [7.22, 7.23] describes the photonuclear absorption as a giant resonance excitation at low energies, and a quasideuteron mechanism at higher energies. In the case of the quasideuteron regime, the initial interaction produces particle-hole excitations and initiates a preequilibrium cascade. We follow Blann's prescription of treating the initial configuration as a $2p$-$1h$ state, to account for correlations in the two hole's degrees of freedom.

Kalbach did not include photonuclear processes in her systematics work. The model described above for angular distributions can be easily applied in this case, using the above formulae. In comparison to nucleon-induced reactions, photonuclear preequilibrium emission would be expected to be less forward-peaked due to the small momentum that a photon carries. Refs. [7.22, 7.23] shows comparisons between this model and experimental data.

Alternatively, it has been shown [7.2] that the above physical principles can be used to adapt Kalbach's nucleon-induced systematics for photon projectiles, by modifying the forward-

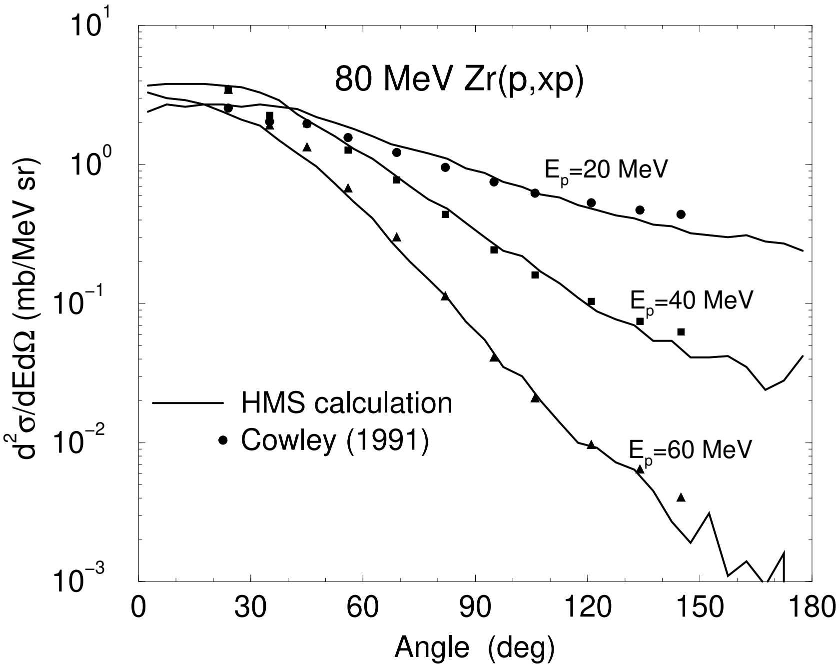

Figure 7.2: Comparison of measured (p,xp) continuum angular distributions with the theory of Ref. [7.3] applied within a Monte Carlo hybrid model context. Data from Cowley *et al.* [7.20]. Taken from Ref. [7.4].

peaking a-parameter. This approach, described in detail in Ref. [7.2], is incorporated into the RIPL **kalbach_systematics.for** code.

Finally, we stress that this approach cannot be applied in the Giant Dipole Resonance region, where a dipole-shaped angular distribution is often observed experimentally.

7.3 Formats

KALBACH_SYSTEMATICS.FOR:

1st Line:	Ac, Zc, Za, Na, Zb, Nb
2nd Line:	Einc
3rd Line:	Nem
Next Nem Lines:	Eem, dxs, fmsd

Where:

Ac, Zc	are the A and Z values for the compound nucleus (before any particle emission occurs).
Za, Na	are the projectile Z and N values.
Zb, Nb	are the ejectile Z and N values.
Einc	is the projectile lab incident energy in MeV.

Nem	is the number of emission energies considered.
Eem, dxs, fmsd	are the emission energy in MeV, the angle-integrated (energy-differential) cross section at this emission energy in mb/MeV, and the preequilibrium fraction (use fmsd=1 as a rough guidance for all but the very low energies) at this emission energy, respectively.

Note that photonuclear reactions in the quasideuteron regime are assumed when Za=Na=0.

LOSALAMOS_ANALYTICAL.FOR:

1st Line:	ein, eout, bindin, bindout, efermi, dsde, amass
2nd Line:	nstages
Next nstages Lines:	rat(i)

Where:

ein, eout	are the incident and emission energies in MeV.
bindin and bindout	are the separation energies for projectile and ejectile from the composite nucleus, in MeV.
efermi	is the Fermi energy (35 MeV).
dsde	is the angle-integrated preequilibrium cross section at emission energy eout.
amass	is the target A value.
nstages	is the number of preequilibrium stages to be included.
rat(i)	is the relative contribution of the preequilibrium stage i to the total preequilibrium spectrum, for emission energy eout.

7.4 Conclusions and Recommendations

The Kalbach systematics provide an invaluable tool for predicting angular distributions in evaluation work since they have a high degree of predictability, they are computationally straightforward to apply, and they are fairly comprehensive in describing most projectile/ejectile types of interest in applications. On the other hand, the Chadwick-Obložinský theory is useful for nuclear model calculations and evaluations since: (a) it is grounded in theory and explains many features of the phenomenological systematics; (b) it can be applied to reactions not considered by Kalbach, for instance photonuclear reactions in the quasideuteron regime; and (c) the model provides a different angular distribution for each preequilibrium step of the reaction and includes the physically-expected behavior of a decrease in forward-peaking as the system moves towards equilibrium.

Our recommendations are:
For nuclear data evaluations, for nucleon reactions up to approximately 200 MeV and for photonuclear reactions in the 40-140 MeV range, continuum angular distributions can be determined with the Kalbach systematics as incorporated in the **kalbach_systematics.for** code.
If an analysis based on a fundamental physical derivation is required, we recommend use of the Chadwick-Obložinský theory [7.3, 7.4] for preequilibrium angular distributions, as implemented in the **losalamos_analytical.for** code.

References

[7.1] C. Kalbach, Phys. Rev. **C37**, 2350 (1988).

[7.2] M.B. Chadwick, P.G. Young and S. Chiba, J. Nucl. Sci. Tech. **32**, 1154 (1995).

[7.3] M.B. Chadwick and P. Obložinský, Phys. Rev. **C50**, 2490 (1994).

[7.4] M. Blann and M.B. Chadwick, "New precompound decay model: Angular distributions", to be published in Physical Review C (1998).

[7.5] Sun Ziyang, Wang Shunuan, Zhang Jingshang, Zhou Yizhong, Z. Phys. **A305**, 61 (1982).

[7.6] C. Costa, H. Gruppelaar and J.M. Akkermans, Phys. Rev. **C28**, 587 (1983).

[7.7] A. Iwamoto and K. Harada, Nucl. Phys. **A419**, 472 (1984).

[7.8] M. Blann, W. Scobel and E. Plechaty, Phys. Rev. **C30**, 1493 (1984).

[7.9] P. Mädler and R. Reif, Nucl. Phys. **A337**, 445 (1980).

[7.10] M.B. Chadwick and P. Obložinský, Phys. Rev. **C44**, R1740 (1991)

[7.11] M.B. Chadwick and P. Obložinský, Phys. Rev. **C46**, 2028 (1992)

[7.12] E. Gadioli and P.E. Hodgson, *Pre-equilibrium Nuclear Reactions* (Clarendon Press, Oxford 1992).

[7.13] H. Feshbach, Phys. Rev. **C48**, R2553 (1993).

[7.14] K. Kikuchi and M. Kawai, *Nuclear Matter and Nuclear Reactions* (North-Holland, Amsterdam 1968), p. 44; M.L. Goldberger, Phys. Rev. **74**, 1269 (1948).

[7.15] F.C. Williams, Nucl. Phys. **A166**, 231 (1971); E. Běták and J. Dobeš, Z. Phys. **A279**, 319 (1976).

[7.16] G. Reffo and M. Herman, Nuovo Cimento Lett. **34**, 261 (1982).

[7.17] K. Sato, Phys. Rev. **C32**, 647 (1985).

[7.18] P.G. Young, E.D. Arthur and M.B. Chadwick, Report LA-12343-MS (Los Alamos National Laboratory 1992).

[7.19] A. Galonsky, R.R. Doering, D.M. Patterson and H.W. Bertini, Phys. Rev. **C14**, 748 (1976).

[7.20] A.A. Cowley, A. van Kent, J.J. Lawrie, S.V. Fortsch, D.M. Whittal, J.V. Pilcher, F.D. Smit, W.A. Richter, R. Lindsay, I.J. van Heerden, R. Bonetti and P.E. Hodgson, Phys. Rev. **C43**, 678 (1991).

[7.21] A. Marcinkowski, R.W. Finlay, G. Randers-Pehrson, C.E. Brient, R. Kurup, S. Mellema, A. Meigooni and R. Taylor, Nucl. Sci. Eng. **83**, 13 (1983).

[7.22] M.B. Chadwick and P.G. Young, "Photonuclear reactions in the GNASH code: Benchmarking model calculations for reactions on lead up to 140 MeV", Lawrence Livermore National Laboratory Document UCRL-ID-118721 (1994).

[7.23] M.B. Chadwick and P.G. Young, Acta Phys. Slov. **45**, 633 (1995).